International Journal of Applied Pharmaceutics

ISSN- 0975-7058 Vol 14, Issue 2, 2022

Original Article

BI-LAMINATED ORAL DISINTEGRATING FILM FOR DUAL DELIVERY OF PITAVASTATIN CALCIUM AND LORNOXICAM: FABRICATION, CHARACTERIZATION AND PHARMACOKINETIC STUDY

MAHMOUD H. TEAIMA[1*], KHALED M. ABDEL-HALEEM[2], MOHAD OSAMA[2], MOHAMED A. EL-NABARAWI[1], SAHAR M. FAYEZ[2]

[1]Department of Pharmaceutics and Industrial Pharmacy, Faculty of Pharmacy, Cairo University, Cairo, Egypt, [2]Department of Pharmaceutics and Industrial Pharmacy, Faculty of Pharmacy, October 6 University, Giza, Egypt
[*]Email: mahmoud.teaima@pharma.cu.edu.eg

Received: 06 Nov 2021, Revised and Accepted: 12 Jan 2022

ABSTRACT

Objective: Pitavastatin calcium (PT) is an innovative drug of statins that enhances HDL-C and lowers LDL-C. However, myalgia has been reported in hyperlipidemic patients receiving statins. Therefore, co-administration of statins with NSAIDs such as Lornoxicam (LN) could be a solution to the former problem. Accordingly, this study aimed to formulate a bi-laminated oral disintegrating film (ODF) comprising PT in one layer and LN in the second one.

Methods: For the formulation and optimization of PT-ODFs, a $3^1.2^1$ full factorial design was carried out, where the impact of polymer type and concentration on disintegration time (DT) and % PT released after 10 min (Q_{10}) was studied. PT-ODFs were prepared *via* the solvent casting method and then evaluated. One PT-ODF was chosen to represent the optimum formula according to the criteria of scoring the fastest DT and the highest Q_{10}. The optimized PT-ODF was merged with the second film layer containing LN, forming a bi-laminated ODF named S1 that underwent an *in vivo* pharmacokinetic study compared to the commercially available tablets for PT (Lipidalon®) and LN (Lornoxicam®) using rats as an animal model. LC-MS/MS was used to analyze plasma drug concentrations.

Results: All PT-ODFs showed acceptable outcomes. F1 scored the fastest DT (18.6±1.5 s) and the highest Q_{10} (91.3±3.0 %). S1 successfully recorded a maximum plasma concentration (C_{max}) of 2.04 and 2.24 folds increase for PT and LN, correspondingly, compared to commercially available tablets.

Conclusion: Merging PT and LN into bi-laminated ODF was promising for the fast delivery of both drugs with enhanced bioavailability.

Keywords: Bi-laminated, Oral disintegrating film, Pitavastatin calcium, Lornoxicam, Liquid chromatography-mass spectrometry

DOI: https://dx.doi.org/10.22159/ijap.2022v14i2.43534. Journal homepage: https://innovareacademics.in/journals/index.php/ijap

INTRODUCTION

Statins are a class of drugs that act against low-density lipoprotein cholesterol (LDL-C), triglycerides and help to enhance high-density lipoprotein cholesterol (HDL-C) in the blood, such as pitavastatin calcium (PT), which is categorized as a novel drug of statins. However, discontinuation of statins is commonly detected among patients due to the incidence of numerous side effects, the most common of which is myalgia [1-4]. Therefore, co-administration of nonsteroidal anti-inflammatory drugs (NSAIDs) with statins can support the treatment of the previously mentioned side effects [5]. NSAIDs are commonly used in the management of muscle pain [6]. One of these NSAIDs is lornoxicam (LN), which is a potent painkiller and anti-inflammatory drug [7, 8]. Among different administration routes, the oral route continues to be the most effective because it is easy to use, non-invasive, provides an accurate dose and has high patient acceptance. Nevertheless, the incidence of low bioavailability due to the first-pass metabolism is still problematic. So, a novel oral drug delivery system was introduced, which is the oral disintegrating film (ODF), where the oral transmucosal route has attracted special attention as it merged the benefits of the oral route and systemic drug delivery without the first-pass effect [9, 10]. This administration route is appropriate for use, particularly in elderly patients, as they struggle to swallow conventional tablets [11]. The ODF is a thin film that adheres to the tongue of the patient and dissolves instantly *via* saliva, releasing the drug for oro-mucosal absorption. So, using ODF would provide the advantages of fast onset of action accurate dosing, and it didn't need water for administration, which in turn would improve patient compliance [10, 12-14].

The purpose of this study was to formulate, evaluate, and optimize different PT-ODFs. Formulation variables affecting PT-ODF properties were studied by applying a $3^1.2^1$ full factorial design *via* Design-Expert® software version 12. The PT-ODF that was chosen to exemplify the optimum formula was merged with the second film layer containing LN, forming a bi-laminated ODF for controlling myalgia triggered by the overuse of statins. An *in vivo* study in rats was carried out to appraise the pharmacokinetic parameters and relative bioavailability of both drugs (PT and LN) in the bi-laminated ODF compared to the commercially available tablets.

MATERIALS AND METHODS

Materials

Pitavastatin calcium (PT) was gifted by Mash Premiere (New Cairo, Egypt). Lornoxicam (LN) (form II) was a gift sample from Global Napi (6th October City, Egypt). The commercially available tablets for PT (Lipidalon®, 1 mg) and for LN (Lornoxicam®, 4 mg) were gifted by Mash Premiere (New Cairo, Egypt) and Global Napi (6th October City, Egypt), respectively. Pullulan was from Hayashibara Biochemical Laboratories Inc. (Okayama, Japan). Hydroxypropyl methylcellulose (HPMC E15) was from Colorcon Limited (Kent, England). Polyvinyl alcohol (PVA) was from MP Biomedicals (Illkirch, France). Glycerol was received from EL Nasr Pharmaceutical (Cairo, Egypt). Diethyl ether was kindly gifted by El-Goumhouria (Cairo, Egypt). Ammonium acetate and Acetonitrile were from Merck (Darmstadt, Germany). Potassium dihydrogen phosphate and disodium hydrogen phosphate were kindly gifted by EL Nasr Pharmaceutical (Cairo, Egypt). Ethyl acetate was from Merck (Darmstadt, Germany). Torsemide was obtained from Multi-Apex Pharma (Cairo, Egypt).

Methods

Studying the effect of various formulation variables *via* full factorial design

A $3^1.2^1$ full factorial design *via* Design Expert® software version 12 (Stat-Ease, Inc., Minneapolis, MN, USA) was used to investigate two

variables, namely, polymer type (X_1) with three levels (pullulan, PVA, and HPMC) and polymer concentration (X_2) with two levels (50 and 80 mg). As shown in table 1, disintegration time (DT) (Y_1) and the % PT released after 10 min (Q_{10}) (Y_2) were chosen as dependent variables. Six formulae were prepared accordingly, and their composition is displayed in table 2.

Table 1: A $3^1.2^1$ full factorial design used for the optimization of PT-ODFs

Factors (independent variables)		Levels	
X_1: Polymer type	Pullulan	PVA	HPMC
X_2: Polymer concentration [a]	50	80	
Responses (dependent variables)	Desirability constraints		
Y_1: DT (sec.)	Minimize		
Y_2: % PT released after 10 min (Q_{10})	Maximize		

[a]mg/film. PT, pitavastatin calcium; ODFs, oral disintegrating films; PVA, polyvinyl alcohol; HPMC, hydroxypropyl methylcellulose; DT, disintegration time.

Table 2: The composition of PT-ODFs and the bi-laminated ODF containing PT and LN

Formula code	PT-ODFs ingredients (mg)				
	PT	Pullulan	PVA	HPMC	Glycerol
F1	1	50	-	-	10
F2	1	80	-	-	10
F3	1	-	50	-	10
F4	1	-	80	-	10
F5	1	-	-	50	10
F6	1	-	-	80	10

The bi-laminated ODF containing PT and LN ingredients (mg)						
PT layer				LN layer		
Formula code	PT	Pullulan	Glycerol	LN	Pullulan	Glycerol
S1	1	50	10	4	50	10

ODFs, oral disintegrating films; PT, pitavastatin calcium; LN, lornoxicam; PVA, polyvinyl alcohol; HPMC, hydroxypropyl methylcellulose.

Formulation of PT-ODFs

The PT-ODFs were prepared using different polymers (pullulan, PVA, or HPMC) *via* the solvent casting method, where pullulan and HPMC were accurately weighed and soaked in cold distilled water, while PVA was dissolved at 80 °Cin distilled water to form a polymeric solution. Then PT, glycerol, and orange flavor were dissolved in a mixture of ethanol and distilled water (1:1) and added to the previously prepared polymeric solution and stirred till a homogenous solution was formed. The solution was degassed in a sonicator to remove air bubbles, then 25 ml of the solution was transferred into a petri-dish with a diameter of 9.8 cm. To avoid sudden evaporation of the solvent and reduce blistering of the film surface, a funnel was inverted above the petri dish after pouring. The solvent was allowed to evaporate for 24 h for film formation. Then the film was removed and cut to the desired size (2x2 cm) using a sharp razor blade, then enfolded in aluminium foil and left in a desiccator till evaluation [12, 15].

Characterization of PT-ODFs

Visual examination

All prepared PT-ODFs were assessed visually for their color, transparency, smoothness, and softness [16].

Thickness

The thickness of the film was determined *via* a micrometer at five different locations (the center and four corners). The average and standard deviation (SD) were calculated [17-19].

Surface pH

The film was wetted with 0.5 ml of simulated saliva fluid (SSF, pH 6.8) and left for 30 s in a petri dish. The pH was noted *via* a pH meter. The readings were reported as mean±SD [17].

Drug content

The film was dissolved in SSF (pH 6.8) in a 100 ml volumetric flask. The absorbance of the solution was determined spectro-photometrically at λ_{max} = 245 nm using a blank (SSF, pH 6.8) for the calculation of drug content [20].

Folding endurance

The value of folding endurance was assessed by folding the film at the same point till it broke or folding it up to 300 times [15, 21, 22].

***In-vitro* disintegration time**

The test was done by placing the film in a petri dish containing 6 ml of SSF (pH 6.8). The time the film began to disintegrate was noted. The average and SD were calculated [17].

***In vitro* drug release study**

The test was done *via* the USP dissolution system, Distek (Model 2500i Type II, TCS-0500 Scheduler, New Jersey, USA) at 37±0.5 °C and a paddle speed of 50 rpm. It was performed by adhering the film to a glass plate using an adhesive and immersing it in 100 ml of SSF (pH 6.8). At time intervals of 2, 4, 6, 8, 10, 20, and 30 min, aliquots of 5 ml were taken and exchanged with equal volumes of SSF (pH 6.8). The absorbance was determined spectrophotometrically at λ_{max} 245 nm and the % PT released was calculated [15].

Optimization of the prepared PT-ODFs

The results of *in vitro* DT and drug release were analyzed by Design Expert® software version 12. Depending on the desirability constraints of factorial outcomes of dependent variables, DT and Q_{10}. The PT-ODF that recorded the fastest DT and the highest Q_{10} with the highest desirability value was selected as the optimum formula.

Scanning electron microscopy (SEM) of the optimum PT-ODF

The topography and structure of the sectioned surface of the optimum PT-ODF were inspected *via* SEM. The film was transversely cut and the texture was investigated *via* SEM at a voltage of 20 kV. A thin part of the film was cut with a scalpel for the preparation of the cross-section sample [23, 24].

Fourier transform infrared spectroscopy (FT-IR) study

Pure PT, the physical mixture of PT with excipients, pure LN, the physical mixture of PT and LN, and the physical mixture of the optimum PT-ODF with LN were all analyzed by FT-IR (Shimadzu®, Japan) *via* the potassium bromide (KBr) pellet method. 3 mg of sample and 300 mg of KBr were grounded by means of a mortar and

pestle. A small portion of the mixture was compressed at 10 kg/cm in a hydraulic press, resulting in a transparent pellet that was inserted into the sample holder and subjected to scanning in the range of 4000 to 500 cm^{-1} [5, 24].

Second derivative spectrophotometric analysis for instantaneous determination of PT and LN in SSF (pH 6.8)

PT and LN mixtures in SSF (pH 6.8) were prepared. The concentration was detected by measuring the absorbance of each drug in different mixtures at PT and LN wavelengths. The recovery percent (R %) was calculated for each mixture, and the interference degree was identified [25].

Formulation of bi-laminated ODF containing PT and LN

The bi-laminated ODF comprises the optimum PT-ODF layer and the LN-ODF layer. Its composition is shown in table 2. Each layer was formulated separately *via* the solvent casting technique, as mentioned before. One of the two layers was sprayed with a few drops of the casting solvent, followed by pressing the second layer on the sprayed side, forming the bi-laminated ODF named S1, and then it was subjected to air drying for 24 h and checked for complete adhesion between both layers prior to use [21]. A preliminary trial was performed for the preparation of ODF containing both drugs (PT and LN), and it was found that combining two drugs into a single film affected the film elasticity as it showed a low folding endurance value. So, it was preferred to formulate a bi-laminated ODF containing PT in one layer and LN in the second one to ensure film elasticity. The bi-laminated ODF exhibited a folding endurance value of up to 300 folds, which indicated the film elasticity as the higher the folding endurance value, the more elastic the film [26, 27].

Characterization of the bi-laminated ODF containing PT and LN

The characterization tests for the S1 ODF were carried out using the same methodologies as those used for PT-ODFs. The *in vitro* release of PT and LN from S1 ODF was compared to that of the commercially available tablets.

***In vivo* pharmacokinetic study of the bi-laminated ODF containing PT and LN**

In this study, twelve male *Wistar* rats were used. They were haphazardly distributed into two groups, each with six animals weighing between 300-350 g. An ethics committee *(PI 2651)*, Faculty of Pharmacy, Cairo University, Egypt, approved the study protocol. Using a parallel design, group I received S1 formula with a dose of 1 mg/kg [28, 29] for PT and 1.6 mg/kg [30] for LN, and group II received the commercially available tablets with the same doses for PT (1 mg/kg) and LN (1.6 mg/kg) based on rat body weight. The commercially available tablets were grounded in distilled water [27] with 0.9 ml containing (0.3 mg) of PT and 1.2 ml containing (0.48 mg) of LN. The S1 ODF was cut into the desired size, containing the adjusted dose of PT and LN. Each group was accommodated in a well-ventilated cage with a controlled temperature environment, a 12 h light-dark cycle, and a regular laboratory diet with free water access [31]. Before the study, the rats fasted for 12 h. Their oral cavities were cleaned to eradicate any debris prior to placing the bi-laminated ODF on the tongue by tweezers. To aid film disintegration, a slight amount of water (50-200 µl) was added [32]. The rats were fed 4 h after receiving the drug and had unlimited access to water throughout the study. Under light anesthesia by diethyl ether, blood samples (0.5 ml) were collected by a heparinized tube from the retro-orbital venous plexus [33] at time intervals of 0, 0.25, 0.5, 1, 2, 4, 8, 24, and 48 h after dosing. The blood samples were centrifuged instantly at 4000 rpm for 5 min (PLC-012, Gemmy Industrial Corp, Taiwan). Liquid Chromatography-Mass Spectrometry (LC-MS/MS) (Shimadzu®, Japan) was used to analyze the plasma supernatant by a valid LC-MS/MS analysis method [24, 34, 35].

Sample preparation and LC-MS/MS assay of PT and LN

A100 µl of torsemide (internal standard) from a (200 ng/ml) stock solution was added to 0.5 ml rat plasma sample. 4 ml ethyl acetate was used to extract torsemide and plasma samples, which were vortexed for 2 min before being centrifuged at 5000 rpm for 5 min. The supernatant was filtered with a 0.22-µm membrane filter and it was evaporated till dryness *via* a vacuum concentrator. The dried residue was reconstituted in 0.5 ml mobile phase; then a 20 µl aliquot was loaded to LC-MS/MS system (Shimadzu®, Japan) with a triple quadrupole detector API-3200, AB Sciex (Foster, CA, USA) to analyze the plasma concentrations. The isocratic flow rate was 1.0 ml/min. The mobile phase was made up of 80% acetonitrile and 20% 0.01% ammonium acetate. The C18 column (4.6×50 mm, 5 µm diameter; Agilent Zorbax, CA, USA) was used to separate the samples. Analyst software version 1.6 was used to process the analytical data [34].

Pharmacokinetic parameters analysis

The pharmacokinetic parameters of PT and LN in the S1 ODF and the commercially available tablets were analyzed using a non-compartmental model *via* Kinetica® software version 5 [24]. The maximum values of PT and LN plasma concentration (C_{max}), the time to reach C_{max} (T_{max}), half-life ($T_{1/2}$), mean residence time (MRT), area under the curve (AUC_{0-48}), and ($AUC_{0-\infty}$) were calculated. Also, the percent relative bioavailability (Frel%) of the S1 formula compared to the commercially available tablets was calculated:

$$\text{Frel\%} = \left(\frac{AUC_{(0-\infty)T}}{AUC_{(0-\infty)ST}}\right) \times 100$$

Statistical analysis

The statistical software of the statistical package for social sciences (SPSS®) version 26 was used to analyze the outcomes of the characterization tests of PT-ODFs. To determine the significance among the prepared PT-ODFs at *(*p<0.05)* in terms of *in vitro* DT and drug release, a one-way analysis of variance *(ANOVA)* was done, followed by post hoc multiple comparisons using the least square difference (LSD). A parametric one-way *ANOVA* test was applied to reveal the significance or non-significance of the pharmacokinetic results of C_{max}, $AUC_{(0-48)}$, $AUC_{(0-\infty)}$ between the S1 ODF and the commercially available tablets. A non-parametric Kruskal-Wallis test was done to compare the T_{max} data obtained from the S1 ODF and the commercially available tablets *via* SPSS® version 26. The results are significant when *(*p<0.05)*.

RESULTS AND DISCUSSION

Characterization of PT-ODFs

The results of all prepared PT-ODFs are presented in table 3. The films were transparent, colorless, thin, and smooth. The thickness values of the PT-ODFs ranged from 0.13±0.05 mm for F1 to 0.26±0.05 mm for F6. All films showed folding endurance values of up to 300 folds, which indicates good film flexibility [15, 21]. All films had a surface pH close to the salivary pH (6.8), ranging from 6.89±0.09 for F3 to 7.02±0.03 for F1. The assay of drug content of all PT-ODFs was within the compendia specifications as it lies in the range between 94.8±1.8 % for F4 and 100.2±0.9 % for F1, and this indicates the uniform distribution of the drug in the film [15].

Influence of formulation variables on DT

Table 3 shows the DT results of PT-ODFs, where the fastest DT was scored by F1 (18.6±1.5 s), while the longest DT was scored by F6 (76.3±0.5 s). The effect of polymer type (X_1) and polymer concentration (X_2) on the DT is shown in fig. 1. The statistical analysis revealed that the polymer type (X_1) exhibited a significant impact on DT *(*p<0.05)*. Pullulan-based ODFs recorded the shortest DT [36]. This might be due to the fact that pullulan is a water-soluble polymer that erodes rapidly, forming pores filled with the solvent diffusing into the film, causing it to disintegrate faster [37,38]. Conversely, HPMC-based ODFs recorded the longest DT. This could be attributed to the fact that HPMC is a viscous film-forming polymer that promotes the formation of a thick gel fluid when the film is in contact with the medium, leading to disintegration hindrance [39]. Concerning polymer concentration (X_2), it significantly influenced the DT *(*p<0.05)*. ODFs containing 50 mg recorded a shorter DT than those containing 80 mg. This could be due to the fact that, as the polymer concentration increased, the film thickness also increased. As a result, the time taken for the disintegration of the film increased, and this was in harmony with Raza *et al.*; Esim *et al.* [40, 41].

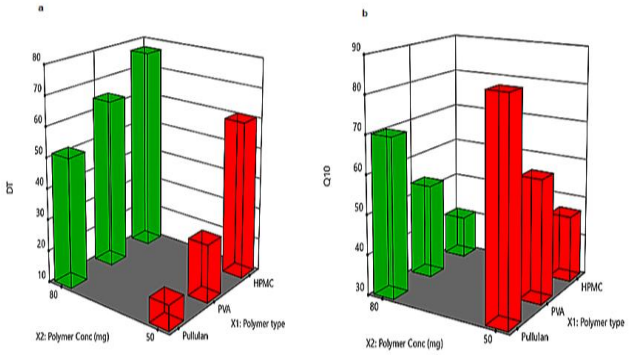

Fig. 1: 3D surface plots for the effect of polymer type (X_1), polymer concentration (X_2) on (a) DT and (b) Q_{10}

Influence of formulation variables on Q10

Fig. 2 displays the *in vitro* release profile of PT from the prepared ODFs. The highest Q_{10} was recorded by F1 (91.3±3.0 %), while the lowest Q_{10} was recorded by F6 (52.8±2.4 %) as shown in table 3. The impact of polymer type (X_1) and polymer concentration (X_2) on Q_{10} is shown in fig. 1. The statistical analysis showed that the polymer type (X_1) significantly influenced Q_{10} *(*p<0.05)*. Pullulan-based ODFs showed the highest Q_{10}. As mentioned earlier, this might be credited to the fact that pullulan is a water-soluble polymer that increases wettability and water permeation into the film matrix, promoting the creation of pores and channels on the surface of the film, resulting in increased drug release [38, 42]. While HPMC-based ODFs recorded the lowest Q_{10}, this could be due to the viscous nature of HPMC, which promotes the creation of a thick gel fluid upon contact with the medium, as previously mentioned, resulting in a delay of drug release from the film [43]. Regarding polymer concentration (X_2), it significantly influenced Q_{10} *(*p<0.05)*. ODFs formulated using 50 mg showed a higher Q_{10} than those prepared using 80 mg. This might be due to that as the polymer concentration decreased, the % drug released increased, as the release of the drug would be less hindered by the polymeric matrix, and this was in accordance with Alsofany *et al.* [44].

Optimization of the prepared PT-ODFs

The Design Expert® software version 12 was an effective way to choose the optimum formula. The software selected the F1 formula, which had the fastest DT (18.6±1.5 s) and the highest Q_{10} (91.3±3.0 %) with overall desirability of 0.985 as the optimum formula.

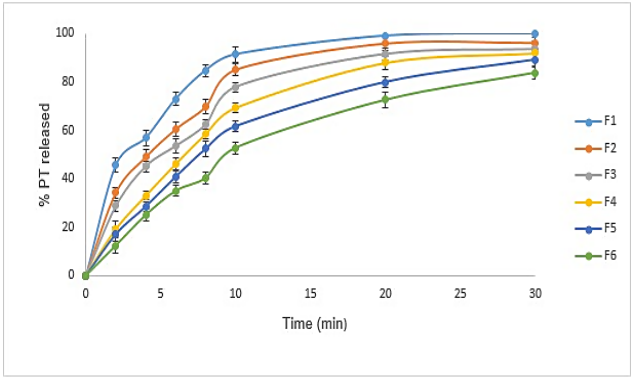

Fig. 2: *In vitro* release profile of PT from ODFs in SSF (pH 6.8), data are presented as mean value±SD, n=3

SEM of the optimum PT-ODF

The SEM of the cross-sectional view of the optimum PT-ODF (F1) is displayed in fig. 3. The micrograph showed that the film had large, deep, and diffusible pores. These pores formed channels through which the water penetrated, facilitating film disintegration and drug diffusion. This was confirmed by the previous outcomes of *in vitro* DT and drug release [45].

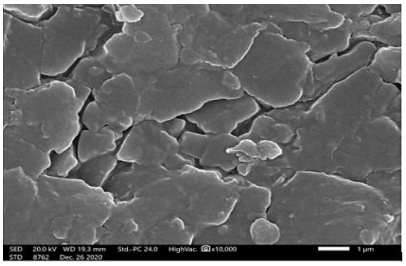

Fig. 3: Scanning electron micrograph (SEM) of the optimum F1 ODF (Magnification X 10.000)

FT-IR

Fig. 4 shows the FT-IR spectra of pure PT, the physical mixture of PT with excipients, pure LN, the physical mixture of PT and LN, and the physical mixture of the optimum PT-ODF with LN (S1 formula). The main peaks of PT are at 1411.06 cm^{-1}, 1554.46 cm^{-1}, 2937.06 cm^{-1}, 3350.30 cm^{-1}, and 3864.50 cm^{-1} owing to its functional groups (C=C, C=O, C-H, O-H, and N-H), respectively [5, 46]. The major peaks of PT were detected in the physical mixture of PT with excipients, indicating the absence of incompatibility. LN showed characteristic peaks at 3053.20 cm^{-1}(–NH) and 1630.63 cm^{-1} (C═O). Other peaks at 1589.81 cm^{-1} and 1529.59 cm^{-1} due to (N–H) group. Peaks due to the (O═S═O) group at 1137.27 cm^{-1}, 1376.08 cm^{-1}, and 1316.67 cm^{-1}. Additional peaks were noticed at 828.40 cm^{-1} (–CH) and 779.73 cm^{-1} (C–Cl) [5, 34]. The main peaks of PT and LN in their physical mixture and in the S1 formula physical mixture persisted in their positions, representing the lack of incompatibility.

Second derivative spectrophotometric analysis for instantaneous determination of PT and LN in SSF (pH 6.8)

At λ_{max} 376 nm of LN, PT had no reading; it gave zero absorption. As a result, there was no interference for measuring LN in the presence

of PT. Conversely, there was a reading for LN at λ_{max} 245 of PT, indicating that there was overlapping between PT and LN as shown in fig. 5. To measure PT in the presence of LN, second derivative method was done. The absorbance and second derivative spectra were recorded for both drugs in SSF pH 6.8: A suitable wavelength was observed *via* the zero-crossing method. The spectra showed that the zero-crossing of LN was at 246.2 nm as shown in fig. 6. The R % was (95.1±0.3 % to 101.5±0.5 %) for PT and (96.7±0.5 % to 102.6±0.2 %) for LN. The interference degree was determined from the R% of the mixtures. There was no interference observed [5].

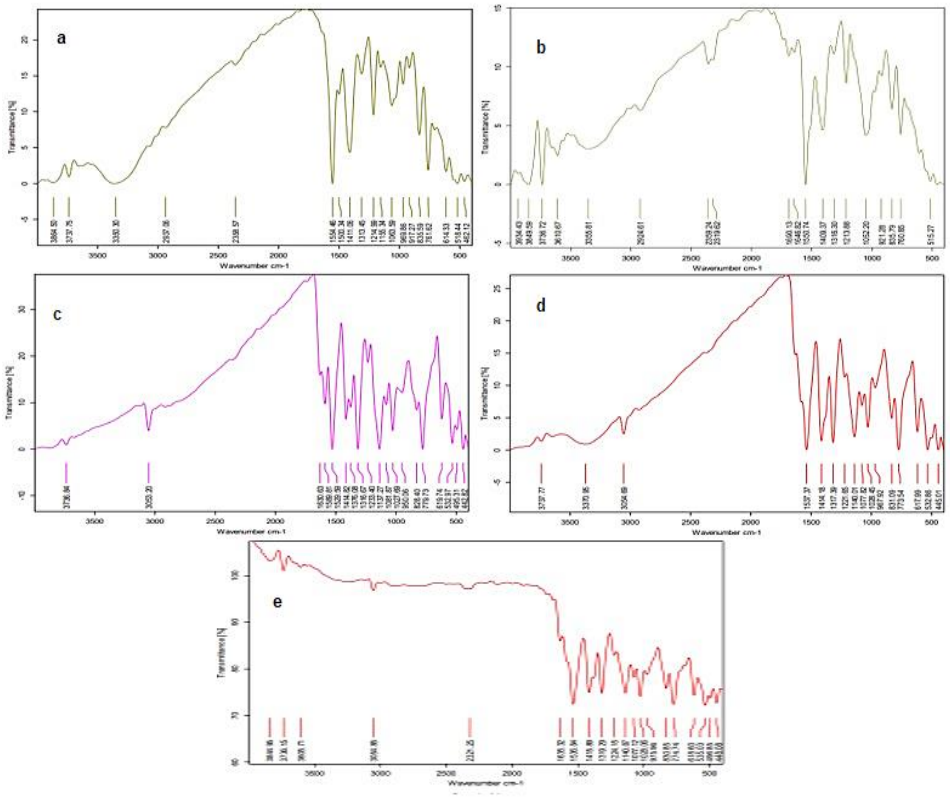

Fig. 4: Fourier transform infrared spectroscopy (FT-IR) spectra of (a) pure PT, (b) physical mixture of PT with excipients (c) pure LN, (d) physical mixture of (PT/lN), and (e) S1 formula physical mixture

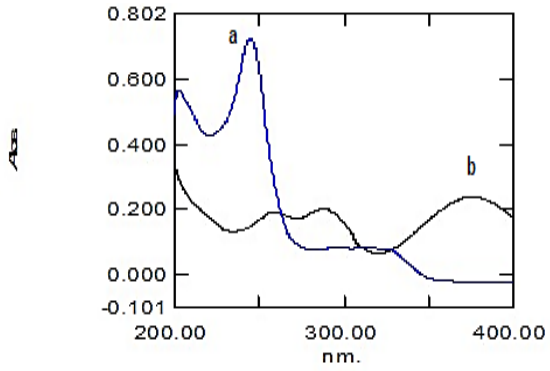

Fig. 5: UV spectra overly of (a) PT and (b) LN in SSF (pH 6.8)

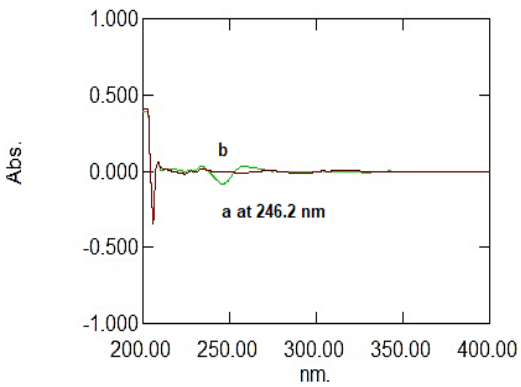

Fig. 6: Second derivative spectra of (a) PT and (b) LN in SSF (pH 6.8)

Characterization of the bi-laminated ODF containing PT and LN

Table 3 displays the results of the characterization tests done on the S1 ODF, where it exhibited a folding endurance value of up to 300 folds which indicates the flexibility of the bi-laminated ODF. The drug content assay was within the compendia specifications. Fig. 7 shows the *in vitro* release profile of PT and LN from S1 and the commercially available tablets, where Q_{10} was 90.21±2.3 % and 83.06±2.4 % for PT and LN, correspondingly, in S1 ODF, and this was higher than the commercially available tablets that recorded Q_{10} of 54.58±1.9 % for PT and 47.72±2.17 % for LN.

Pharmacokinetic parameters analysis

Table 4 and fig. 8 show that the mean value of C_{max} of the S1 ODF and C_{max} of the commercially available tablets were significantly different *(*p<0.05),* with 2.04 and 2.24 folds increase regarding PT and LN, correspondingly, compared to the commercially available tablets. The statistical analysis revealed that the mean value of T_{max} of S1 was significantly shorter *(*p<0.05)* than the commercially available tablets. The mean value of AUC $_{(0-\infty)}$ of S1 was 2.3 times for PT and 2.14 times for LN, which was significantly *(*p<0.05)* greater than that of commercially available tablets. Additionally, the Frel% of S1

was 230.04 % for PT and 214.02 % for LN with respect to the commercially available tablets. The results of T_{max}, AUC $_{(0-\infty)}$, and Frel% showed that S1 ODF attained good sound results compared to the commercially available tablets. The enhanced bioavailability and the faster absorption rate of the two drugs, as marked by higher C_{max} and faster T_{max} compared to the commercially available tablets, might be due to that the drug was partially absorbed *via* the oral mucosa [12]. Additionally, the fast absorption of both drugs from S1 correlates well with the *in vitro* drug release results, where PT and LN showed rapid release from S1 ODF.

Table 3: Characterization of PT-ODFs and the bi-laminated ODF containing PT and LN

Formula	Thickness (mm)	Surface PH	Folding endurance (No of folds)	Drug content (%)		DT (sec)	Q_{10} (%)	
PT-ODFs								
F1	0.13±0.05	7.02±0.03	298.6±1.1	100.2±0.9		18.6±1.5*	91.3±3.0*	
F2	0.23±0.05	6.98±0.03	295.6±1.5	98.92±0.7		51.6±1.1	85.1±2.5	
F3	0.14±0.05	6.89±0.09	299.6±0.5	96.20±1.7		28.3±0.6	77.8±2.0	
F4	0.24±0.05	6.99±0.02	294.3±0.5	94.80±1.8		64.3±1.5	69.3±2.1	
F5	0.16±0.05	6.91±0.08	299.6±0.5	98.03±1.0		60.6±1.1	61.6±2.2	
F6	0.26±0.05	6.96±0.07	296.6±1.5	95.50±1.3		76.3±0.5	52.8±2.4	
	The bi-laminated ODF containing PT and LN							
				PT	LN		PT	LN
S1	0.2±0.05	7.01±0.02	296.2±0.5	98.90±0.5	97.63±1.0	23.6±1.0	90.21±2.3	83.06±2.4

Data are presented as mean value±SD, n=3. *F1 is significantly different compared to the other formulae F2-F6 at *p<0.05.* ODFs, oral disintegrating films; DT, disintegration time; PT, Pitavastatin calcium; LN, Lornoxicam.

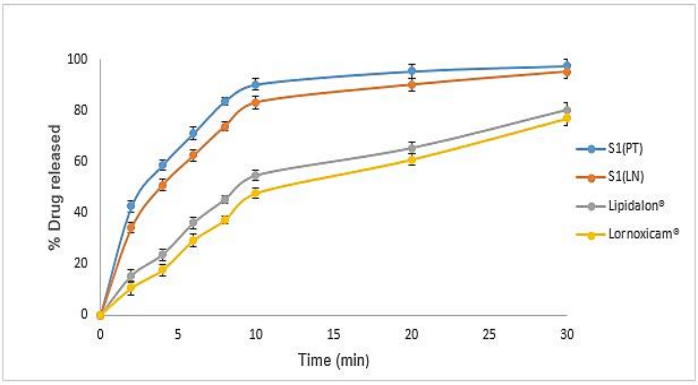

Fig. 7: *In vitro* release profile of PT and LN from S1 ODF and the commercially available tablets in SSF (pH 6.8), data are presented as mean value±SD, n=3

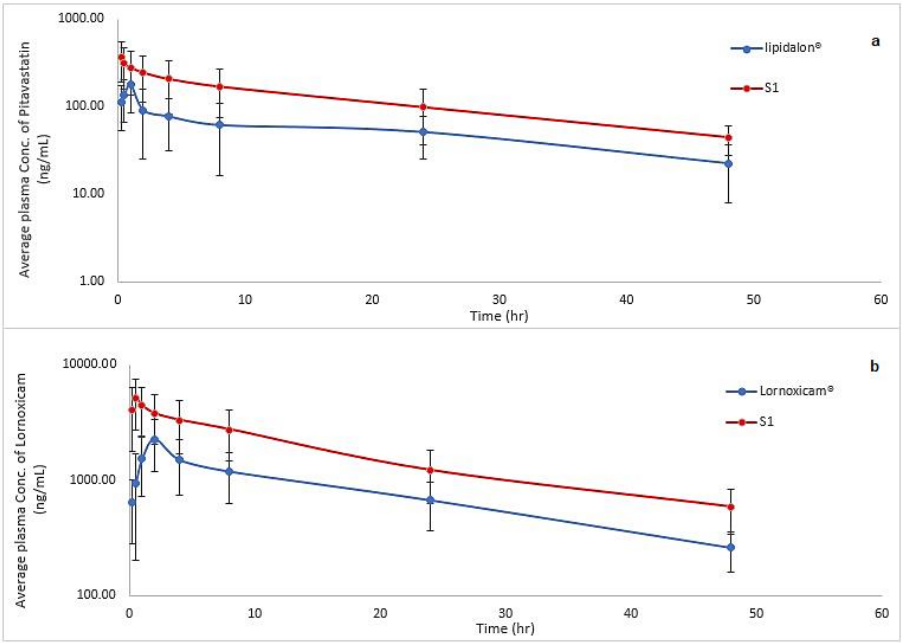

Fig. 8: Mean plasma concentration profiles of (a) PT from S1 and lipidalon®, (b) LN from S1 and lornoxicam® after oral administration, data are presented as mean value±SD, n=6

Table 4: The pharmacokinetic parameters and relative bioavailability of the bi-laminated ODF compared to the commercially available tablets

	S1(PT)	S1(LN)	Lipidalon®	Lornoxicam®
C_{max} (ng/ml)	430.551±89.122*	6109.283±451.031*	210.793±47.311	2725.862±323.239
T_{max} (h)	0.25±0.00*	0.417±0.129*	0.875±0.306	1.833±0.408
MRT (h)	15.385±1.625	14.812±0.849	16.324±0.878	15.529±0.924
$T_{1/2}$ (h)	18.267±4.612	17.23±2.782	20.368±4.757	18.478±2.854
AUC_{0-48} (ng. h/ml)	6318.121±2284.21*	94151.611±11956.232*	2711.85±1160.346	44046.117±3662.818
$AUC_{0-\infty}$ (ng. h/ml)	7507.391±2572.589*	111288.938±13866.471*	3263.461±1385.042	51998.344±4458.253
Frel%	230.04	214.02	-	-

Data are presented as mean value±SD, n=6. *S1 is significantly different compared to the commercially available tablets at $p<0.05$. C_{max}, maximum plasma concentration; T_{max}, time to reach maximum plasma concentration; MRT, mean residence time; $T_{1/2}$, half-life; AUC, area under the curve; Frel%: percent relative bioavailability; PT, pitavastatin calcium; LN, lornoxicam; ODF, oral disintegrating film.

CONCLUSION

A $3^1.2^1$ full factorial design was applied to choose the optimum PT-ODF. F1 prepared using pullulan at a concentration of 50 mg showed good sound results in terms of DT and Q_{10}. Merging PT and LN was successfully done *via* the formulation of the bi-laminated ODF, comprising both drugs to support the treatment of myalgia caused by statin overuse. The *in vivo* pharmacokinetic study revealed that the bi-laminated ODF (S1) was found to be optimal for delivering the two drugs with enhanced bioavailability and a faster absorption rate with respect to the commercially available tablets. Nevertheless, further clinical pharmacokinetic and pharmacodynamic studies are needed to confirm the attained results and to verify that the co-administration of PT and LN can treat myalgia induced by statin overuse.

STATEMENT OF ANIMAL RIGHTS

The Institutional Animal Ethics Committee *(PI 2651),* Faculty of Pharmacy, Cairo University, Egypt, approved the study protocol.

FUNDING

Nil

AUTHORS CONTRIBUTIONS

All the authors have contributed equally.

CONFLICT OF INTERESTS

No conflict of interest was declared by the authors.

REFERENCES

1. Lestari S, Soegianto L, Hermanu LS. Potensi antibakteri dan antibiofilm ekstrak etanol bunga bintaro (*Cerbera odollam*) terhadap staphylococcus aureus ATCC 6538 fakultas farmasi, [Unika widya mandala surabaya antibacterial and antibiofilm potential of the ethanolic extract of suicide tree]. J Pharm Sci Prac. 2017;4:30-5.
2. O'Toole GA, Kaplan HB, Kolter R. Biofilm formation as microbial development. Annu Rev Microbiol. 2000;54:49-79. doi: 10.1146/annurev.micro.54.1.49, PMID 11018124.
3. Karatan E, Watnick P. Signals, regulatory networks, and materials that build and break bacterial biofilms. Microbiol Mol Biol Rev. 2009;73(2):310-47. doi: 10.1128/MMBR.00041-08, PMID 19487730.
4. Kining E, Falah S, Nurhidayat N. The *in vitro* antibiofilm activity of waterleaf extract of papaya (*Carica papaya* L.) against *Pseudomonas aeruginosa*. Curr Biochem. 2016;2(3):150-63. doi: 10.29244/cb.2.3.150-163.
5. Risal G, Shrestha A, Kunwar S, Paudel G, Dhital R, Budha MB, Nepal R. Detection of biofilm formation by Escherichia coli with its antibiogram profile. Int J Community Med Public Health. 2018;5(9):3771. doi: 10.18203/2394-6040.ijcmph20183562.
6. Chakotiya AS, Tanwar A, Narula A, Sharma RK. Alternative to antibiotics against Pseudomonas aeruginosa: effects of *Glycyrrhiza glabra* on membrane permeability and inhibition of efflux activity and biofilm formation in *Pseudomonas* aeruginosa and its *in vitro* time-kill activity. Microb Pathog. 2016;98:98-105. doi: 10.1016/j.micpath.2016.07.001. PMID 27392698.
7. Hidayati NA, Christiani C. Peran biofilm terhadap infeksi saluran ginjal yang disebabkan oleh vaginosis bakterial. Predical Derm Vener. 2019;31(2).
8. Archer NK, Mazaitis MJ, Costerton JW, Leid JG, Powers ME, Shirtliff ME. Staphylococcus aureus biofilms: properties, regulation, and roles in human disease. Virulence. 2011;2(5):445-59. doi: 10.4161/viru.2.5.17724, PMID 21921685.
9. Donlan RM. Role of biofilms in antimicrobial resistance. ASAIO J. 2000;46(6):S47-52. doi: 10.1097/00002480-200011000-00037, PMID 11110294.
10. Ming D, Wang D, Cao F, Xiang H, Mu D, Cao J, Li B, Zhong L, Dong X, Zhong X, Wang L, Wang T. Kaempferol inhibits the primary attachment phase of biofilm formation in staphylococcus aureus. Front Microbiol. 2017 Nov 15;8:2263. doi: 10.3389/fmicb.2017.02263, PMID 29187848.
11. Patel N, Oudemans PV, Hillman BI, Kobayashi DY. Use of the tetrazolium salt MTT TO measure cell viability effects of the bacterial antagonist *Lysobacter enzymogenes* on the filamentous fungus *Cryphonectria parasitica*. Antonie Leeuwenhoek. 2013;103(6):1271-80. doi: 10.1007/s10482-013-9907-3, PMID 23529159.
12. Kumara INC, Sri Pradnyani IGA, Sidiarta I, Kunyit UEE. (*Curcuma longa*) terhadap daya hambat pertumbuhan bakteri streptococcus mutans. Intisari Sains Medis. 2019;10:462-7.
13. Barus SH, Hamidah S, Satriadi T, Kehutanan J. Uji fitokimia senyawa aktif tumbuhan manggarsih (*Parameria laevigata* (Juss.) Moldenke) dari hutan alam desa malinau loksado dan hasil budidaya eksitu banjarbaru. J Sylva Scienteae. 2019;2:510-8.
14. Depkes R. Inventaris tanaman obat indonesia III. Jakarta: Badan Penelitian Pengembangan Kesehatan; 1994. p. 183-4.
15. Herlina W. Kitab tanaman obat nusantara. Jakarta: media Pressindo; 2011. p. 806-7.
16. Muharrami LK, Munawaroh F, Ersam T. Inventarisasi tumbuhan jamu dan skrining fitokimia kabupaten sampang. Pena Sains. 2017;4:124-32.
17. Pemanfaatan SR, Kunyit EK. (*Curcuma domestica*) sebagai indikator titrasi asam basa. Teknoin. 2016;22:595-601.
18. Kolasa LC. Uji daya antimikroba ekstrak n-heksan kulit kayu repeat (*Parameria laevigata* (Juss.) Moldenke) terhadap pertumbuhan bakteri escherichia coli dengan kloramfenikol. Universitas Surabaya; 2008.
19. Saludarez M. Anti-bacterial and anti-inflammatory property evaluation *of Parameria laevigata* (Lupiit) for the formulation of an ointment. Int J Adv Res 2019;7(6):488-96. doi: 10.21474/IJAR01/9248.
20. Gurevitch J, Koricheva J, Nakagawa S, Stewart G. Meta-analysis and the science of research synthesis. Nature. 2018;555(7695):175-82. doi: 10.1038/nature25753, PMID 29517004.
21. Selçuk AA. A guide for systematic reviews: PRISMA. Turk Arch Otorhinolaryngol. 2019;57(1):57-8. doi: 10.5152/tao.2019.4058, PMID 31049257.
22. Snyder H. Literature review as a research methodology: an overview and guidelines. J Bus Res. 2019;104:333-9. doi: 10.1016/j.jbusres.2019.07.039. jbusres.2019.07.039.
23. Arciola CR, Campoccia D, Ravaioli S, Montanaro L. Polysaccharide intercellular adhesin in biofilm: structural and regulatory aspects. Front Cell Infect Microbiol. 2015;5:7. doi: 10.3389/fcimb.2015.00007. PMID 25713785.

24. Archer NK, Mazaitis MJ, Costerton JW, Leid JG, Shirtliff M. Staphylococcus aureus biofilms: properties, regulation, and roles in human disease. Virulence. 2011;2:45-59.
25. Sharma V, Sharma C, Sharma S. Influence of *Curcuma longa* and curcumin on blood profile in mice subjected to aflatoxin b1. IJPSR. 2014;7:90-100.
26. Kostakioti M, Hadjifrangiskou M, Hultgren SJ. Bacterial biofilms: development, dispersal, and therapeutic strategies in the dawn of the postantibiotic era. Cold Spring Harb Perspect Med. 2013;3(4):a010306. doi: 10.1101/Csh Perspect.a010306, PMID 23545571.
27. Rabin N, Zheng Y, Opoku Temeng C, Du Y, Bonsu E, Sintim HO. Biofilm formation mechanisms and targets for developing antibiofilm agents. Future Med Chem. 2015;7(4):493-512. doi: 10.4155/fmc.15.6, PMID 25875875.
28. Gunardi WD. Mekanisme biomolekuler pseudomonas aeruginosa dalam pembentukan biofilm dan sifat resistensi terhadap antibiotika. J Kedokteran Meditek. 2017;22:1-7.
29. Jamal M, Hussain T, Das CR, Andleeb S. Characterization of siphoviridae phage Z and studying its efficacy against multidrug-resistant klebsiella pneumoniae planktonic cells and biofilm. J Med Microbiol. 2015;64(4):454-62. doi: 10.1099/jmm.0.000040.
30. Taghadosi R, Shakibaie MR, Masoumi S. Biochemical detection of N-acyl homoserine lactone from biofilm-forming uropathogenic escherichia coli isolated from urinary tract infection samples. Rep Biochem Mol Biol. 2015;3(2):56-61. PMID 26989738.
31. Satpathy S, Sen SK, Pattanaik S, Raut S. Review on bacterial biofilm: an universal cause of contamination. Biocatalysis and Agricultural Biotechnology. 2016;7:56-66. doi: 10.1016/j.bcab.2016.05.002.
32. Hamidah S, HF ST, Hasil Budidaya FA, Banjarbaru E. Fakultas Kehutanan universitas lambung Mangkurat; 2016.
33. Muharrami LK, Munawaroh F, Ersam T, Santoso M. Phytochemical screening of ethanolic extract: a preliminary test on five medicinal plants on Bangkalan. J Pena Sains. 2020;7(2):96-102. doi: 10.21107/jps.v7i2.8722.
34. Hayat S, Sabri AN. Screening for antibiofilm and antioxidant potential of turmeric (*Curcuma longa*) extracts. Pak J Pharm Sci. 2016;29(4):1163-70. PMID 27393429.
35. Suhartono S, Ismail YS, Muhayya SR. The interference of *Moringa oleifera* leaf extracts to modulate quorum sensing-facilitated virulence factors. Biodiversitas. 2019;20(10):3000-4. doi: 10.13057/biodiv/d201031.
36. Dewatisari WF. Perbandingan variasi pelarut dari ekstrak daun lidah mertua (*Sansevieria trifasciata*) terhadap rendemen dan aktivitas antibakteri. Seminar Nasional Pendidikan Biologi & Saintek. 2019;4:292-300.
37. Nugroho SW, Rukmo M, Prasetyo EA, Yuanita T, Buah Kakao AEK. (*Theobroma cacao*) 6,25% dan NaOCl 2,5% terhadap bakteri streptococcus sanguinis. J Conserv Dent J 2019;9:19.
38. da Silva Negreiros Neto T, Gardner D, Hallwass F, Leite AJM, de Almeida CG, Silva LN, de Araujo Roque A, de Bitencourt FG, Barbosa EG, Tasca T, Macedo AJ, de Almeida MV, Giordani RB. Activity of pyrrolizidine alkaloids against biofilm formation and trichomonas vaginalis. Biomed Pharmacother. 2016;83:323-9. doi: 10.1016/j.biopha.2016.06.033. PMID 27399809.
39. Sun J, Wu J, An B, de Voogd NJ, Cheng W, Lin W. Bromopyrrole alkaloids with the inhibitory effects against the biofilm formation of gram-negative bacteria. Marine Drugs. 2018;16(1). doi: 10.3390/md16010009, PMID 29301295.
40. Agustina W, Handayani D. Skrining fitokimia dan aktivitas antioksidan beberapa fraksi dari kulit batang jarak (Ricinus communis L.). J Pendidikan Ilmu Kimia. 2017;1:117-22.
41. Cosmo Andrade J, da Silva ARP, Audilene Freitas M, de Azevedo Ramos B, Sampaio Freitas T, de Assis G Dos Santos F, Leite Andrade MC, Nunes M, Relison Tintino S, da Silva MV, Dos Santos Correia MT, de Lima Neto RG, Neves RP, Melo Coutinho HD. Control of bacterial and fungal biofilms by natural products of Ziziphus joazeiro mart. (Rhamnaceae). Comp Immunol Microbiol Infect Dis. 2019;65:226-33. doi: 10.1016/j.cimid.2019.06.006. PMID 31300118.
42. Primasari A, Nasution M, Hidayati Arbi NH, Sari DP, Basyuni M. The effectiveness of soursop leaf extract against growth of aggregatibacter actinomycetemcomitans ATCC® 6514TM *in vitro*. Asian J Pharm Clin Res. 2018;11(12):411-5. doi: 10.22159/ajpcr.2018.v11i12.28435.
43. da Silva Negreiros Neto T, Gardner D, Hallwass F, Leite AJM, de Almeida CG, Silva LN, de Araujo Roque A, de Bitencourt FG, Barbosa EG, Tasca T, Macedo AJ, de Almeida MV, Giordani RB. Activity of pyrrolizidine alkaloids against biofilm formation and trichomonas vaginalis. Biomed Pharmacother. 2016;83:323-9. doi: 10.1016/j.biopha.2016.06.033, PMID 27399809.
44. Bhunu B, Mautsa R, Mukanganyama S. Inhibition of biofilm formation in mycobacterium smegmatis by parinari curatellifolia leaf extracts. BMC Complement Altern Med. 2017;17(1):1–10:285. doi: 10.1186/s12906-017-1801-5, PMID 28558683.
45. Sadowska B, Budzyńska A, Wieęckowska Szakiel M, Paszkiewicz M, Stochmal A, Moniuszko Szajwaj B, Kowalczyk M, Rożalska B. New pharmacological properties of medicago sativa and saponaria officinalis saponin-rich fractions addressed to candida albicans. J Med Microbiol. 2014;63(8):1076-86. doi: 10.1099/jmm.0.075291-0, PMID 24850879.
46. Von Borowski RG, Zimmer KR, Leonardi BF, Trentin DS, Silva RC, de Barros MP, Macedo AJ, Gnoatto SCB, Gosmann G, Zimmer AR. Red pepper capsicum baccatum: source of antiadhesive and antibiofilm compounds against nosocomial bacteria. Ind Crops Prod. 2019;127:148-57. doi: 10.1016/j.indcrop.2018.10.011.
47. Sari A, Widyarman, Wendhita WIP, Tjakra EE, Murdono FI, Binartha CTO. Review article prevention and treatment of white spot lesions in orthodontic patients. Contemp Clin Dent. 2020;10:123-8.
48. Andriani Y, Mohamad H, Bhubalan K, Abdullah MI, Amir H. Phytochemical analyses, anti-bacterial and anti-biofilm activities of mangrove-associated hibiscus tiliaceus extracts and fractions against *Pseudomonas* aeruginosa. J Sustain Sci Manag. 2017;12:45-51.
49. Di Marco NI, Pungitore CR, Lucero Estrada CSM. Aporphinoid alkaloids inhibit biofilm formation of yersinia enterocolitica isolated from sausages. J Appl Microbiol. 2020;129(4):1029-42. doi: 10.1111/jam.14664, PMID 32279402.
50. Radita DC, Widyarman AS, Dewa M. (God's crown) fruit extract inhibits the formation of periodontal pathogen biofilms *in vitro*. J Indones Dent Assoc. 2019;2:57.